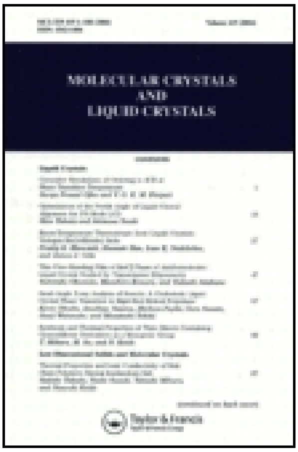

Molecular Crystals and Liquid Crystals Incorporating Nonlinear Optics
Publication details, including instructions for authors and subscription information:
http://www.tandfonline.com/loi/gmcl17

Chemistry of the Doping Mechanism in $Ba_{1-x}K_xBiO_3$ and $La_2CuO_{4+\delta}$ Oxide Superconductors

D. G. Hinks [a], J. D. Jorgensen [a], D. R. Richards [a], B. Dabrowski [a], Ying Zheng [b] & Shlyou Pei [a]

[a] Materials Science Division, Argonne National Laboratory, Argonne, IL, 60439

[b] University of Wisconsin, Milwaukee, WI, 53201

To cite this article: D. G. Hinks, J. D. Jorgensen, D. R. Richards, B. Dabrowski, Ying Zheng & Shlyou Pei (1990): Chemistry of the Doping Mechanism in $Ba_{1-x}K_xBiO_3$ and $La_2CuO_{4+\delta}$ Oxide Superconductors, Molecular Crystals and Liquid Crystals Incorporating Nonlinear Optics, 184:1, 39-49

To link to this article: http://dx.doi.org/10.1080/00268949008031737

Mol. Cryst. Liq. Cryst., 1990, vol. 184, pp. 39–49
Reprints available directly from the publisher
Photocopying permitted by license only

Printed in the United States of America

CHEMISTRY OF THE DOPING MECHANISM IN $Ba_{1-x}K_xBiO_3$ AND $La_2CuO_{4+\delta}$ OXIDE SUPERCONDUCTORS

D. G. HINKS, J. D. JORGENSEN, D. R. RICHARDS, B. DABROWSKI, *YING ZHENG, AND SHLYOU PEI
Materials Science Division, Argonne National Laboratory, Argonne, IL 60439 and
*University of Wisconsin, Milwaukee, WI 53201

Abstract The chemistry involved in doping oxide materials to form metallic, superconducting compounds can be far from simple. Recent work on two materials, $Ba_{1-x}K_xBiO_3$ and $La_2CuO_{4+\delta}$, show the range of complex chemistry involved.

INTRODUCTION

All oxide superconductors are doped insulators. Understanding the nature of the doping mechanism is difficult because of the low dopant concentration necessary to induce metallic behavior and eventually, superconductivity. Thus, we are at the limit of our analytical sensitivity to detect the small changes in stoichiometry which occur and, furthermore, at the limit of our knowledge of the fundamental oxide chemistry which determines the extent and nature of the doping mechanism.

Some systems, such as $YBa_2Cu_3O_{7-\delta}$, are at least qualitatively understood. Although the details of the variation of T_c with oxygen content are not totally explained, the structure and chemistry of the defect system, involving an oxygen site which can support a wide range of occupancy, are on a firm footing. Conversely, the defect structure of the bismuth- and thallium-based copper-oxide materials is still far from understood. The complex nature of these multicomponent systems, with many possible intrinsic defects (e.g. interstitial oxygen, cation nonstoichiometry, metal-ion intersite exchange, etc.) is the subject of extensive research.

In this paper we discuss two simple systems for which the chemistry is becoming clear. For each system a very different aspect of oxide chemistry determines the doping mechanism which induces superconductivity. In $Ba_{1-x}K_xBiO_3$, the doping of potassium into the parent compound, $BaBiO_3$, requires the careful control of oxygen partial pressure. With oxygen at atmospheric pressure, little potassium can be incorporated into the lattice. At elevated temperatures in low partial pressures of oxygen, an oxygen-deficient vacancy phase in which potassium is soluble is formed. Annealing this potassium-containing material at low temperature in oxygen fills the oxygen vacancies, producing a superconducting material. Thus, in this system, oxygen stoichiometry controls the doping mechanism although oxygen, by itself, does not control the superconductivity. Interstitial oxygen is soluble in $La_2CuO_{4+\delta}$. Near room temperature this excess oxygen separates into a phase containing about 0.08 excess oxygen ions per formula unit and a phase containing nominally no excess oxygen. The oxygen-rich phase is superconducting while the stoichiometric one is an antiferromagnetic insulator. This phase separation (which requires oxygen diffusion near room temperature) was totally unexpected and opens a new avenue for oxide chemistry in these materials.

POTASSIUM DOPING IN THE $Ba_{1-x}K_xBiO_3$ SYSTEM

Superconductivity in the Ba-K-Bi-O system was first discovered by Mattheiss et al.[1] Cava et al.[2] were the first to prepare the pure compound and identify the structure as a simple cubic perovskite, $Ba_{1-x}K_xBiO_3$. The initial synthesis procedure was thought to depend on the generation of high oxygen partial pressures and was done in sealed silver tubes with a large excess of KO_2. It was subsequently shown by Hinks et al.[3,4] that the incorporation of potassium required low oxygen pressures to reduce the parent compound. After the potassium was incorporated into the reduced material, the oxygen vacancies could be filled at a lower temperature in flowing oxygen.

Fig. 1 shows a typical thermogravimetric analysis (TGA) curve for an x=0.375 sample. Heating in nitrogen causes an oxygen loss which corresponds to the reduction of the bismuth to a trivalent oxidization state. The potassium is incorporated into the lattice under these conditions. After cooling in nitrogen, the material is oxidized in flowing oxygen at about 425° C to yield a superconducting material with stoichiometric oxygen content. Heating the material in oxygen to temperatures above 425° C, as shown in Fig. 2, causes an irreversible loss of potassium from the compound. The resulting material contains the potassium doped compound, $Ba_{1-x}K_xBiO_3$, with less potassium then the starting composition, and $KBiO_2$. The weight-loss data can be used to calculate the solubility of potassium in the perovskite compound as a function of temperature at 1 atm oxygen partial pressure according to the equation:

$$Ba_{1-z}K_zBiO_3 = (z-x)/(1-x)KBiO_2 + (1-z)/(1-x)Ba_{1-x}K_xBiO_3 + (z-x)/2(1-x)O_2 ,$$

where z is the starting composition (0.375 for the data shown) and x is the final composition (or the solubility in this case).

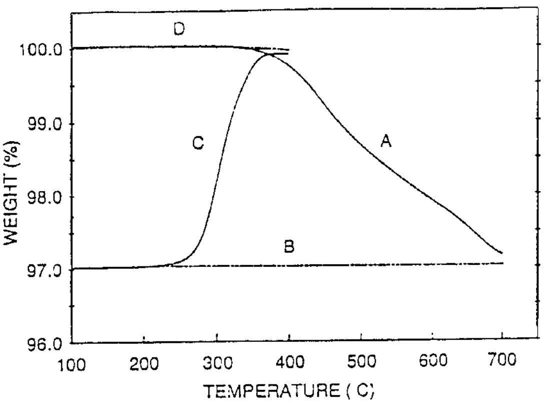

Figure 1 TGA curve for a $Ba_{0.623}K_{0.375}BiO_3$ sample in N_2 (A, heat:B, cool) followed by O_2 (C,heat: D,cool).

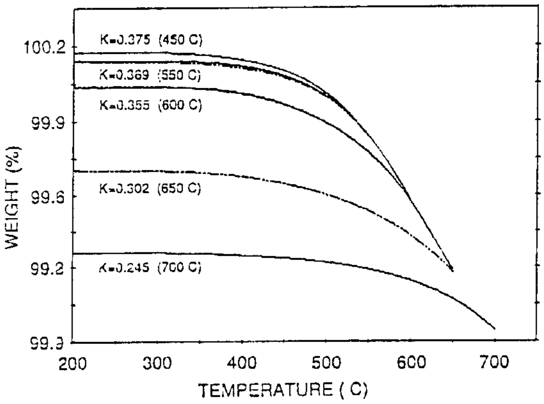

Figure 2 Weight loss for a $Ba_{0.623}K_{0.375}BiO_3$ sample heated and cooled to successively higher temperatures in pure O_2. The numbers indicate the solubility of K at each firing temperature.

Fig. 3A shows the diffraction pattern for a sample with a potassium content of 0.2 synthesized under the same conditions as used for material with compositions greater than 0.375 (i.e. nitrogen at 700° C followed by oxygen at 400° C). The material has phase separated into two compounds, one with x> 0.2 and one with x<0.2. We found that to prepare single-phase material with x less than 0.375 it is necessary to react the material in a slightly oxidizing environment. For example, at x=0.2, the potassium is incorporated at 800° C in 8% oxygen. Fig. 3B shows diffraction data for a sample prepared under these conditions. The material has sharp diffraction peaks as shown by the $K_{\alpha 1}$-$K_{\alpha 2}$ separation. We conclude that each composition in the phase diagram will, in principle, require a different oxygen partial pressure and firing temperature to avoid phase separation at compositions below x=0.375 and allow the desired solubility of potassium.

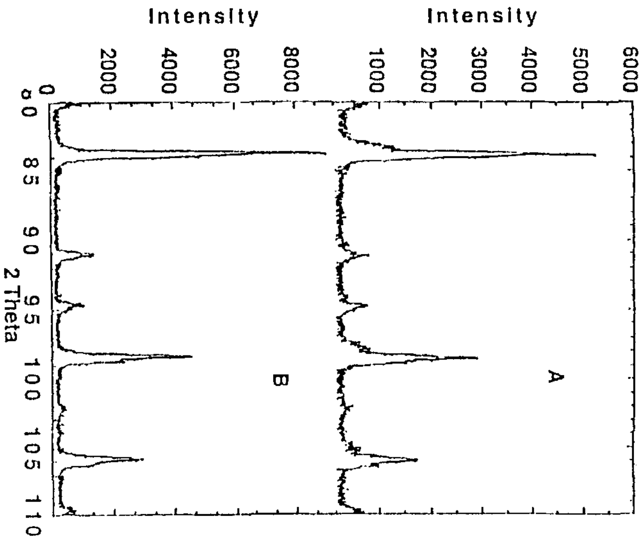

Figure 3 Diffraction pattern for a $Ba_{0.8}K_{0.2}BiO_3$ sample synthesized by A) firing in N_2 or B) firing in 8% O_2 at 800° C in each case followed by O_2 annealing at 400° C.

Understanding the chemistry involved during the high-temperature synthesis step requires "in situ" analysis. We have recently begun these studies using neutron powder diffraction at Argonne's Intense Pulsed Neutron Source. Fig. 4 shows a sequence of diffraction patterns for an x=0.4 sample as the material is heated in flowing argon containing 1% oxygen. Between 560 and 600° C an impurity phase (identified as $KBiO_2$)

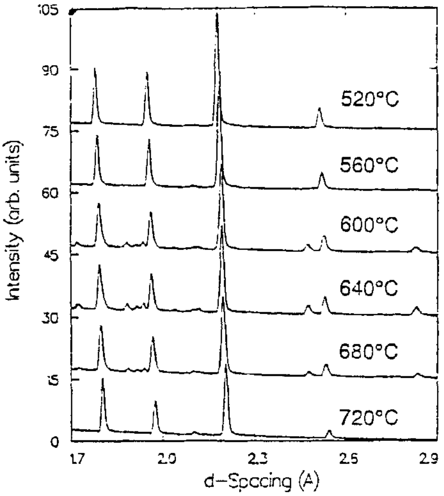

Figure 4 In situ neutron diffraction patterns on heating in flowing 1% O_2.

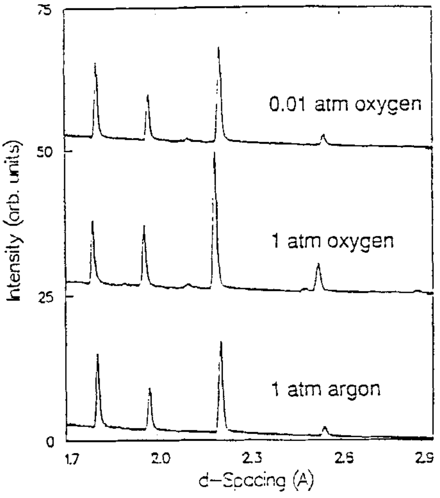

Figure 5 In situ neutron diffraction patterns at 720° C in different atmospheres.

appears and above 680^0 C the $KBiO_2$ is reincorporated into the $Ba_{1-x}K_xBiO_3$ compound. If flowing nitrogen is used as the gas environment, no $KBiO_2$ is formed. However, in 1% oxygen at about 600° C the solubility of potassium was exceeded, leading to the precipitation of $KBiO_2$. At higher temperatures, as the vacancy concentration increases, the potassium solubility increases and potassium is reincorporated into the $Ba_{1-x}K_xBiO_3$ compound. At 720° C, the solubility of potassium is greater than $x=0.4$ in 1% oxygen; however, in pure oxygen, $KBiO_2$ again precipitates out of the material as shown in Fig. 5.

As the single-phase $x=0.4$ material is cooled in flowing argon, a phase transition is observed near 600° C as shown in Fig. 6. This new phase is an oxygen-deficient vacancy-ordered compound whose structure is shown in Fig. 7. The structure is a $\sqrt{2}a \times 2\sqrt{2}a \times a$ supercell of the simple cubic perovskite lattice (with lattice constant **a**). The oxygen vacancies in the basal plane are fully ordered on the O4 site, as shown in Fig. 7b. In addition, the oxygen atom sites above and below the plane (O1) are only 70% occupied, giving an overall composition of $Ba_{0.6}K_{0.4}BiO_{2.2\,\pm 0.1}$. Thus, at high temperature, the potassium is incorporated into a disordered cubic structure, maintaining a nominal Bi oxidization state of 3. On cooling, the oxygen vacancies order, leading to the observed supercell. Fig. 8 shows the final heating to 400° C in flowing oxygen. The oxygen vacancies are filled and the material converts to the simple cubic perovskite structure.

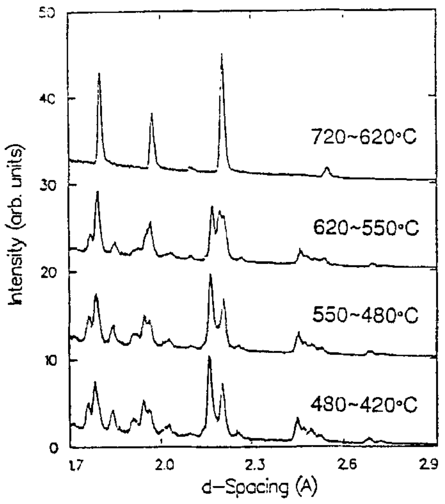

Figure 6 In situ neutron diffraction patterns on cooling in flowing argon.

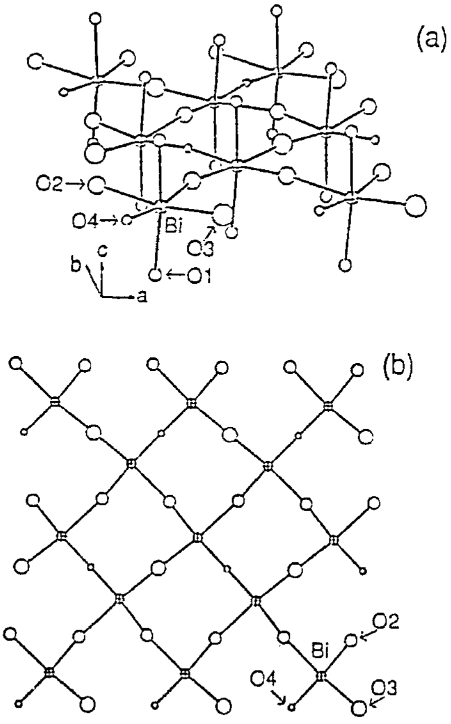

Figure 7 Structure of the vacancy-ordered $Ba_{0.6}K_{0.4}BiO_{2.2}$ compound. The distorted BiO_6 network is shown in (a), the Ba(K) atoms have been left out for clarity. The basal plane is shown in (b).

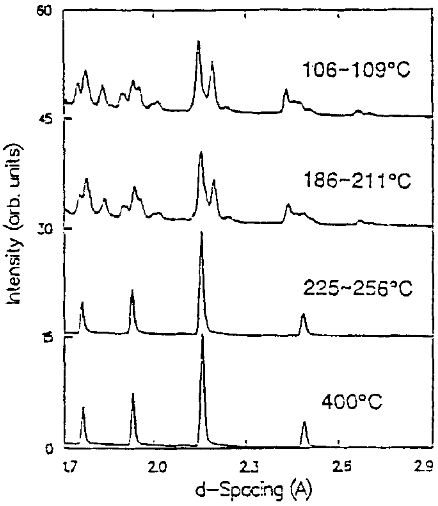

Figure 8 In situ neutron diffraction patterns on heating the vacancy-ordered phase in flowing oxygen.

Table 1 lists the structural parameters found for the vacancy-ordered compound. In situ diffraction studies are now underway with samples containing less potassium in the region of the phase diagram where phase separation occurs, in order to understand this phenomena.

Table 1. Structural parameters for the vacancy-ordered oxygen deficient phase at 130°C. Space group is orthorhombic Pba2 (#32) with a=6.127 Å, b=12.016 Å and c=4.378 Å with Z=4. Numbers without errors were not fit.

atom	site	x (Å)	y (Å)	z (Å)	occupancy
Ba-K	4c	0.806(1)	0.138(1)	-0.056(8)	2.4-1.6
Bi	4c	0.283(1)	0.114(1)	0.467(7)	4
01	4c	0.299(2)	0.116(1)	-0.040(9)	2.72(4)
02	4c	0.71(1)	0.246(1)	0.509(9)	4.00(8)
03	2a	0	0	0.5	2.08(4)
04	2b	0	0.5	0.5	0.12(8)

INTERSTITIAL OXYGEN IN La_2Cu0_4

The observation of traces of superconductivity in "pure" La_2Cu0_4 [5-7] posed a perplexing question beginning shortly after the discovery of superconductivity in the Sr doped compound by Bednorz and Muller.[8] Material annealed in nitrogen shows semiconducting behavior, but samples prepared in oxygen-containing environments show traces of superconductivity.[9] A sample synthesized in 25 kbar of oxygen shows metallic conductivity and complete diamagnetic shielding.[10]

High-resolution neutron diffraction showed that samples annealed at moderate oxygen pressures contained two phases, both with orthorhombic structures and nearly degenerate lattice constants.[11] Fig. 9 shows the lattice constants as a function of temperature for a sample processed in 0.1kbar of oxygen.[11] Above 425K the sample is single phase with the known tetragonal structure. The material becomes orthorhombic (space group Bmab) at about 425K in agreement with the literature. However, near 300K phase separation occurs. At this point the excess oxygen initially dissolved uniformly in the material segregates into a phase containing approximately 4.08 oxygen atoms per formula unit (the Fmmm phase), leaving a nearly stoichiometric (Bmab) phase. The amount of superconductivity scales with the volume fraction of Fmmm phase.

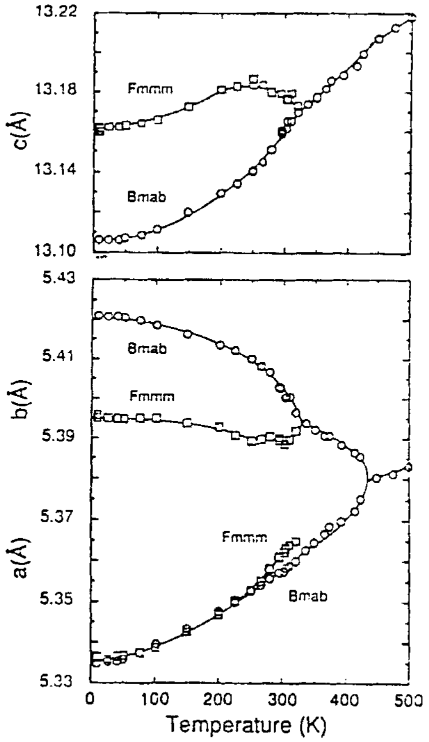

Figure 9 Lattice constants as a function of temperature for a $La_2CuO_{4+\delta}$ sample annealed in 0.1 kbar oxygen.

The structure of the excess-oxygen defect was determined for the isostructural compound $La_2NiO_{4+\delta}$, where the solubility of excess oxygen is much greater.[12] Fig. 10 shows the defect structure. The excess oxygen is situated at an interstitial site as an oxide ion almost tetrahedrally coordinated to four nearest-neighbor La ions. This defect can dope the CuO_2 planes with holes analogous to the doping obtained by the substitution of divalent Sr ions for trivalent La ions. Since the superconducting transition temperatures observed in $La_{1.85}Sr_{0.15}CuO_4$ and $La_2CuO_{4.08}$ are the same (about 35K) the concentration of carriers must be similar. Indeed, the substitution of 0.16 Sr ions for La (0.16 carriers per unit formula) would be equivalent to doping with 0.08 interstitial oxide ions, a concentration consistent with our observed concentration of oxide ions in the Fmmm phase.

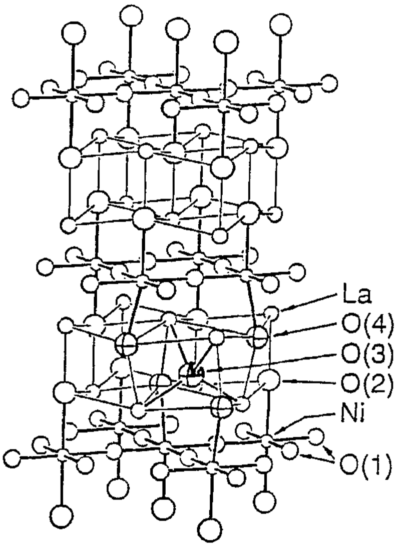

Figure 10 Structure of the interstitial oxygen defect in $La_2CuO_{4+\delta}$.

CONCLUSIONS

In the systems described the nature of the electronically active dopant is different and the method of introducing the dopant requires much different chemistry. Understanding the solid-state chemistry of the superconducting oxides is one of the most important tasks facing the chemist since only by understanding the chemistry of these materials will new, hopefully better, oxide superconductors be found.

ACKNOWLEDGMENTS

This work was supported by the National Science Foundation-Office of Science and Technology Centers under Contract # DMR-88-09854 (BD, SP) and the U.S. Department of Energy, BES, under contract # W-31-109-ENG-38 (DGH,JDJ,YZ). One of us (DRR) would like to thank American Air Liquide for financial support.

REFERENCES

1. L.R. Mattheiss, E.M. Gyorgy, and D.W. Johnson Jr., Phys.Rev., B 37, 3745, (1988).
2. R.J. Cava, B. Batlogg, J.J. Krajewski, R.C. Farrow, L.W. Rupp, Jr., A.E. White, K.T. Short, W.F. Peck, Jr., and T.Y. Kometani, Nature, 332, 814 (1988).
3. D.G. Hinks, B. Dabrowski, J.D. Jorgensen, A.W. Mitchell, D.R. Richards, Shiyou Pei, and Donglu Shi, Nature, 333, 836, (1988).
4. D.G. Hinks, D.R. Richards, B. Dabrowski, A.W. Mitchell, J.D. Jorgensen, and D.T. Marx, Physica C, 156, 477 (1988).
5. P.M. Grant, S.S.P. Parkin, V.Y. Lee, E.M. Engler, M.L. Ramirez, G. Lim, and R.D. Jacowitz, Phys. Rev. Lett., 58, 2482 (1987).
6. J. Beille, R. Cabanel, C. Chaillout, B. Chevalier, G. Demazeau, F. Deslandes, J. Etourneau, P. Lejay, C. Michel, J. Provost, B. Raveau, A. Sulpice, J.-L. Tholence, and R. Tournier, C. R. Acad. Sc. Paris Ser., 2, 304, 1097 (1987).
7. K. Sekizawa, Y. Takano, H. Takigami, S. Tasaki, and T. Inaba, Jpn. J. Appl. Phys., 26, L840 (1987).
8. J.G. Bednorz and K.A. Muller, Z. Phys. B, 64, 198 (1986); S. Uchida, H. Takagi, K. Kitazawa, and S. Tanaka, Jpn. J. Appl. Phys., 26, L1 (1987); H. Takagi, S. Uchida, K. Kitazawa, and S. Tanaka, Jpn. J. Appl. Phys., 26, L123 (1987).
9. B. Dabrowski, D.G. Hinks, J.D. Jorgensen and D.R. Richards, Mat. Res. Soc. Symp. Proc., 156,77 (1989).
10. B. Dabrowski, J.D. Jorgensen, D.G. Hinks, Shiyou Pei, D.R. Richards, K.G. Vandervoort, G.W. Crabtree, H.B. Vanfleet and D.L. Decker (to be published in the Proceedings of the Conference on Superconductivity and Applications, 19-21 September 1989, Buffalo New York).
11. J.D. Jorgensen, B. Dabrowski, Shiyou Pei, D.G. Hinks, L. Soderholm, B. Morosin, J.E. Schirber, E.L. Venturini and D.S. Ginley, Phys. Rev. B, 38, 11337 (1988).
12. J.D. Jorgensen, B. Dabrowski, Shiyou Pei, D.R. Richards and D.G. Hinks, Phys.Rev. B, 40, 2187 (1989).